Ti_2Sn_3: A Novel Binary Intermetallic Phase, Prepared by Chemical Transport at Intermediate Temperature

Holger Kleinke,*,† Markus Waldeck,‡ and Philipp Gütlich‡

Department of Chemistry, University of Waterloo, Waterloo, Ontario, Canada N2L 3G1, and Institut für Anorganische Chemie und Analytische Chemie, Johannes-Gutenberg-Universität, D-55128 Mainz, Germany

Received February 14, 2000. Revised Manuscript Received May 4, 2000

Ti_2Sn_3 was obtained by chemical transport using iodine as the transport agent in a sealed quartz ampule at 500 °C. Its crystal structure—a new type structure—was determined via single-crystal structure analysis to be orthorhombic, space group *Cmca*, $a = 595.56(4)$, $b = 1996.4(2)$, $c = 702.81(5)$ pm, $V = 835.6(1) \times 10^6$ pm^3, and $Z = 8$. The structure can be derived from a three-dimensional condensation of a single polyhedron, which comprises a Ti atom in the center, surrounded by seven Sn and four Ti atoms forming a tri-capped square antiprism. Supporting the results of the self-consistent band structure calculations, Ti_2Sn_3 is a metallic *p*-type conductor, exhibiting Pauli paramagnetism and a specific resistivity of 160 $\mu\Omega$ cm at room temperature. ^{119}Sn Mössbauer spectroscopy revealed Ti_2Sn_3 to be a stannide with three chemically slightly different Sn atoms.

Introduction

Our interest in the Ti−Sn and related systems relies on our investigations of polar intermetallics with homonuclear interactions within the cationic as well as anionic substructures[1] and of compounds with potentially mixed valences.[2] In general, the former lead to rather complex crystal structures since at least three different kinds of bonding occur in a given structure, i.e., the often dominating heteronuclear bonds and the two different homonuclear interactions.

A multitude of new stannides of the main group metals A (A = Na, K, Mg, Ca, Sr) have been uncovered in the past few years, all of which exhibit bonds between the Sn atoms in various anionic states, but no A−A bonds. Examples include Na_5Sn_{13},[3] $NaSn_5$,[4] K_8Sn_{25}, K_8Sn_{44},[5] $Ca_{6.2}Mg_{3.8}Sn_7$,[6] $Ca_{31}Sn_{20}$,[7] and $SrSn_3$.[8] The last compound served as an example for a superconductor, the band structure of which exhibits bands with a saddle point at the Fermi level as well as other bands cutting the Fermi level with high dispersions, i.e., localized and itinerant electrons. This coincidence was also observed in the layered high-temperature superconducting cuprates as well as in borocarbides and was subsequently considered to be a chemical fingerprint for superconductivity.[9,10] Because of the tendency of tin to form lone electron pairs, the occurrence of flat bands in the neighborhood of the Fermi level is likely in Sn-rich compounds.

However, although the binary Ti−Sn system has been studied for decades,[11] the most Sn-rich compound in this system known to date is Ti_6Sn_5, a compound which comprises homonuclear Ti−Ti and Sn−Sn bonds.[12] Our explorations revealed the existence of the hitherto unknown compound Ti_2Sn_3, which is introduced in this article, via tackling synthesis, crystal and electronic structure, and physical properties.

Experimental Section

Synthesis and Structure Determination. The most common method to prepare intermetallics is based on heating of the elements at rather high temperatures, i.e., above the melting points. Aside from high-energy costs and often a lack of well-shaped single crystals, this method has a severe disadvantage in systems with constituent elements that exhibit significantly different melting points, such as titanium and tin (melting points: 1670 vs 232 °C). Another method, the chemical transport, uses the phenomenon that solid starting materials may become mobile in the gas phase by means of reversible solid/gas reactions. The crystallization out of the gas phase often enables the formation of excellent and large single crystals. In addition to the application in halogen lamps, the chemical transport is commercially used for ultraclean syntheses of metals, e.g., aluminum, titanium (van Arkel de Boer), and nickel (Mond).[13]

* To whom correspondence should be addressed. E-mail: kleinke@uwaterloo.ca.
† University of Waterloo.
‡ Johannes-Gutenberg-Universität Mainz.

(1) Kleinke, H. *J. Am. Chem. Soc.* **2000**, *122*, 853, and references therein.
(2) Gütlich, P.; Range, K. J.; Felser, C.; Schultz-Münzenberg, C.; Tremel, W.; Walcher, D.; Waldeck, M. *Angew. Chem.* **1999**, *38*, 2381.
(3) Vaughey, J. T.; Corbett, J. D. *Inorg. Chem.* **1997**, *36*, 4316.
(4) Fässler, T. F.; Kronseder, C. *Angew. Chem.* **1998**, *37*, 1571.
(5) Zhao, J.-T.; Corbett, J. D. *Inorg. Chem.* **1994**, *33*, 5721.
(6) Ganguli, A. K.; Corbett, J. D.; Köckerling, M. *J. Am. Chem. Soc.* **1998**, *120*, 1223.
(7) Ganguli, A. K.; Guloy, A. M.; Leon-Escamilla, E. A.; Corbett, J. D. *Inorg. Chem.* **1993**, *32*, 4349.
(8) Fässler, T. F.; Hoffmann, S. *Z. Anorg. Allg. Chem.* **2000**, *626*, 106.
(9) Hirsch, J. E.; Scalapino, D. J. *Phys. Rev. Lett.* **1986**, *56*, 2732.
(10) Simon, A. *Angew. Chem., Int. Ed. Engl.* **1997**, *36*, 1788.
(11) Massalski, T. B. *Binary Alloy Phase Diagrams*, 2nd ed.; ASM International, Materials Park, OH, 1990.
(12) Schubert, K.; Frank, K.; Gohle, R.; Maldonado, A.; Meissner, H. G.; Raman, A.; Rossteutscher, W. *Naturwissenschaft* **1963**, *50*, 41.
(13) Schäfer, H. *Chemische Transportreaktionen*; VCH: Weinheim, 1962.

10.1021/cm000131z CCC: $19.00
Published on Web 07/11/2000

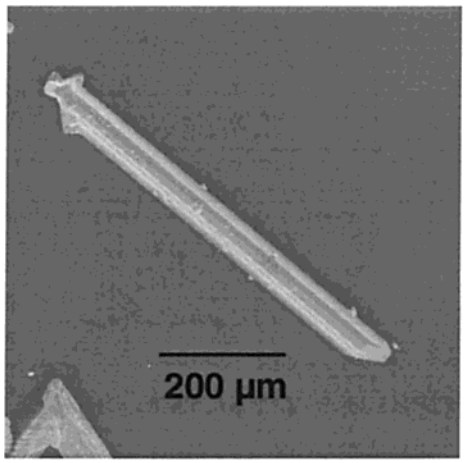

Figure 1. Single crystal of Ti_2Sn_3.

Table 1. Crystallographic Data for Ti_2Sn_3

chemical formula: Ti_2Sn_3	formula weight: 481.87 g/mol
$a = 595.56(4)$ pm	space group: *Cmca* (No. 64)
$b = 1996.4(2)$ pm	$T = 22$ °C; $\lambda = 71.069$ pm
$c = 702.81(5)$ pm	$\rho_{calcd} = 7.184$ g/cm^3
$V = 835.6(1) \times 10^6$ pm^3	$\mu = 211.1$ cm^{-1}
$Z = 8$	$R(F_o)^a = 0.012$; $R_w(F_o^2)^b = 0.025$

^{a} $R(F_o) = \Sigma||F_o| - |F_c||/\Sigma|F_o|$. ^{b} $R_w(F_o^2) = [\ \Sigma[w(F_o^2 - F_c^2)^2]/\Sigma[w(F_o^2)^2]\ ]^{1/2}$.

Binnewies et al. have investigated systematically the chemical transport of intermetallics, including cobalt stannides.[14] Both elements used here, titanium and tin, can be transported with iodine as the transport agent. Titanium and tin form in reversible reactions the halides TiI_4 (boiling point (bp) 377 °C) and SnI_2 (bp 717 °C) in equilibrium with Sn_2I_4 and SnI_4 (bp 365 °C), respectively. We succeeded in preparing the new compound Ti_2Sn_3 by loading the elements in the stoichiometric ratio 2:3 in evacuated silica tubes, followed by heating over a period of 5 days at 500 °C using traces of iodine as the transport agent. This procedure yielded single crystals of Ti_2Sn_3 of considerable length and excellent quality (Figure 1), while melting of both elements in the stoichiometric ratio led to the formation of Ti_6Sn_5 (and unreacted elemental tin). This is deduced to arise from the reversible disproportionation of Ti_2Sn_3 into Ti_6Sn_5 and Sn at 780 °C, as DTA measurements (SETARAM) revealed. However, Ti_2Sn_3 also forms by annealing of the elements at temperatures between 600 and 750 °C in quantitative yields, but not below 550 °C, independent of the particle size of the starting materials. Reactions aiming at Sn-richer compounds have failed so far.

To gain insight into the crystal structure of Ti_2Sn_3, a complete data set from a needle-like single crystal was collected using the imaging plate detector system from STOE. The straightforward structure solution[15] and refinement[16] gave a reasonable structure model in space group *Cmca*, as described below, with satisfying residual factors of $R(F) = 0.012$ and $R_w(F^2) = 0.025$. Crystallographic details may be found in Table 1. Atomic positions and displacement parameters are listed in Table 2.

The composition was confirmed by energy-dispersive analyses of X-rays, performed using an electron microscope (CAMSCAN, CS 4DV) with an additional EDX device (detector: NORAN INSTRUMENTS) on selected crystals. On the basis of Guinier diagrams and (standardless) EDX results, no phase range exists; the Ti:Sn ratio was determined to be 40(2):60.

Table 2. Positional and Equivalent Displacement Parameters

atom	site	x	y	z	U_{eq} (pm^2)
Sn1	8*f*	0	0.22390(1)	0.57434(4)	80.2(8)
Sn2	8*f*	0	0.12139(1)	0.92675(4)	72.1(8)
Sn3	8*e*	1/4	0.02065(1)	1/4	68.7(8)
Ti1	8*f*	0	0.08054(3)	0.54820(9)	57(2)
Ti2	8*e*	1/4	0.16427(3)	1/4	55(1)

Table 3. Parameters Used for Extended Hückel Calculations

orbital	H_{ii} (eV)	ς_1	c_1	ς_2	c_2
Ti, 4s	−6.919	1.50			
Ti, 4p	−3.483	1.50			
Ti, 3d	−6.673	4.55	0.4391	1.600	0.7397
Sn, 5s	−16.16	2.12			
Sn, 5p	−8.32	1.82			

Band Structure Calculations. The extended Hückel theory[17] was used to calculate the Mulliken gross and overlap populations[18] for the different interactions using a mesh of 648 *k* points of the reciprocal primitive unit cell. While the Hückel parameters for Ti and Sn were taken from standard sources,[19] the ionization potentials of Ti were optimized by charge iteration directly on Ti_2Sn_3 (Table 3).

Since the Hückel theory depends strongly on the parameters used, self-consistent tight-binding LMTO calculations (LMTO = linear muffin tin orbitals)[20] were carried out to get more reliable results for the band structure. Therein, the density functional theory is used with the local density approximation (LDA). The integration in *k* space was performed by an improved tetrahedron method[21] on a grid of 1221 irreducible *k* points of the first Brillouin zone. The ASA radii were determined to be 1.588 (Ti1), 1.642 (Ti2), 1.733 (Sn1), 1.640 (Sn2), and 1.684 pm (Sn3). The void space was filled with three so-called empty spheres. Some general differences in the results of Hückel and LMTO calculations were discussed before and were found to occur in this case accordingly.[22]

Physical Property Measurements. Temperature-dependent resistivity measurements between 290 and 10 K were performed on a cold-pressed polycrystalline bar of the dimensions 1.0 × 0.2 × 0.15 cm^3, applying an a.c. four-probe technique. The absolute Seebeck coefficient was determined on the same cold-pressed bar at six different temperature gradients to check for consistency. Magnetic data for a ground polycrystalline sample were collected using a SQUID magnetometer and thereafter corrected for diamagnetic core contributions. ^{119}Sn Mössbauer measurements were carried out at absorber temperatures of 293 and 100 K, with the $Ca^{119}SnO_3$ source being kept at room temperature. A 100-μm Pd foil was used to eliminate the Sn−K radiation of the source.

Results and Discussion

Crystal Structure. Our investigations clearly revealed the existence of the most Sn-rich compound known to date in the binary Ti−Sn system, namely, Ti_2Sn_3. The valence-electron-poor transition metal M:Sn ratio of 2:3 was unambiguously determined, while other stannides earlier identified as M_2Sn_3 (M = V,[23] Nb,[24]

(14) Gerighausen, S.; Binnewies, M. *Z. Anorg. Allg. Chem.* **1995**, *621*, 936; Neddermann, R.; Wartchow, R.; Binnewies, M. *Z. Anorg. Allg. Chem.* **1998**, *624*, 733; Gerighausen, S.; Wartchow, R.; Binnewies, M. *Z. Anorg. Allg. Chem.* **1998**, *624*, 1057.

(15) Sheldrick, G. M. *SHELXS-86*; University of Göttingen, Germany, 1986.

(16) Sheldrick, G. M. *SHELXL-97*; University of Göttingen, Germany, 1997.

(17) Hoffmann, R. *J. Chem. Phys.* **1963**, *39*, 1397; Whangbo, M.-H.; Hoffmann, R. *J. Am. Chem. Soc.* **1978**, *100*, 6093; Program EHMACC, adapted for use on a PC by M. Köckerling, Gesamthochschule Duisburg, 1997.

(18) Mulliken, R. S. *J. Chem. Phys.* **1955**, *23*, 2343.

(19) Clementi, E.; Roetti, C. *At. Nucl. Data Tables* **1974**, *14*, 177.

(20) van Barth, U.; Hedin, L. *J. Phys.* **1971**, *C4*, 2064; Andersen, O. K. *Phys. Rev.* **1975**, *B12*, 3060; Skriver, H. L. *The LMTO Method*; Springer: Berlin, 1984.

(21) Blöchl, P. E.; Jepsen, O.; Andersen, O. K. *Phys. Rev.* **1994**, *B49*, 16223.

(22) Kleinke, H.; Felser, C. *J. Solid State Chem.* **1999**, *144*, 330; Kleinke, H.; Felser, C. *J. Alloys Compd.* **1999**, *291*, 73.

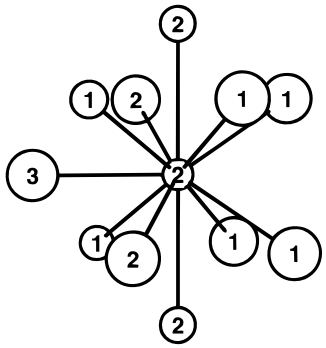

Figure 2. Tricapped square antiprism in the structure of Ti_2Sn_3. Small circles, Ti; large circles, Sn.

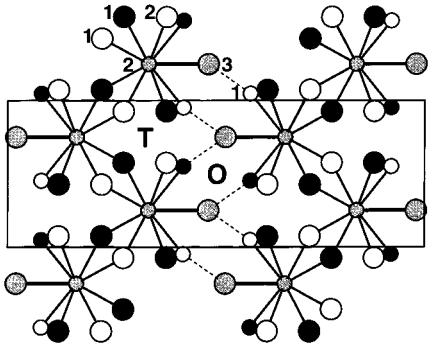

Figure 3. Projection of the structure of Ti_2Sn_3 along [100]. Horizontal: *b* axis. Small circles, Ti; large circles, Sn. The different heights are reflected in different shadings of the atoms.

Cr[25]) have recently been corrected to be monometal distannides, MSn_2.[26] We therefore consider Ru_2Sn_3[27] as the most similar stannide with the same M:Sn ratio, although ruthenium is a valence-electron-rich transition metal.

The Ru_2Sn_3 structure (Ru_2Si_3 type) consists of $RuSn_6$ octahedra interconnected via common edges and corners to the three-dimensional structure. One can also describe the unprecedented Ti_2Sn_3 structure on the basis of a single polyhedron, which consists of one Ti atom (Ti2) surrounded by seven Sn and four Ti atoms, in the form of a tricapped square antiprism, as depicted in Figure 2.

These square antiprisms are interconnected via common faces to a linear chain parallel to [100]. The three-dimensional structure results from a condensation of neighbored chains over common Sn1 atoms and Ti1−Sn3 bonds (dashed lines in Figure 3). This condensation occurs with Sn_4 tetrahedra forming linear chains, again parallel to [100], by a condensation via common edges. The centers of the tetrahedra (**T** in Figure 3) are unoccupied; the distances between the void and the surrounding Sn atoms of 220 pm suggest a possibility to intercalate small atoms. In addition, chains of empty Ti_2Sn_4 octahedra run parallel to the tetrahedra chains, with the centers of the octahedra (marked as **O**) having

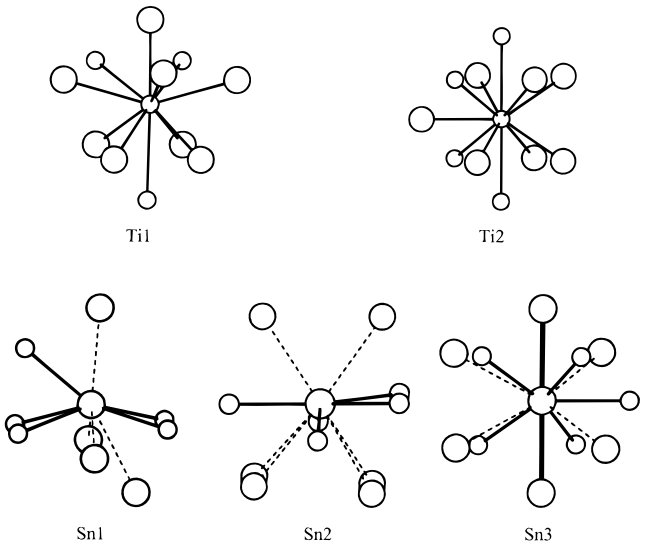

Figure 4. First-coordination spheres of all five atom sites.

Table 4. Interatomic Distances, Mulliken Overlap Populations (MOP), and Pauling Bond Orders (PBO)

interaction	no.	*d* (pm)	MOP	PBO
Ti1−Sn2	1×	278.27(7)	0.372	0.849
Ti1−Sn3	2x	283.52(6)	0.276	0.694
Ti1−Sn1	1×	286.79(7)	0.317	0.612
Ti1−Sn3	2×	288.26(6)	0.219	0.578
Ti1−Sn2	2×	309.25(3)	0.171	0.258
Ti1−Ti2	2×	306.65(6)	0.184	0.195
Ti1−Ti1	1×	328.64(9)	0.100	0.084
Ti2−Sn2	2×	284.80(3)	0.313	0.661
Ti2−Sn3	1×	286.72(7)	0.293	0.614
Ti2−Sn1	2×	295.39(5)	0.258	0.440
Ti2−Sn1	2×	297.15(4)	0.252	0.411
Ti2−Ti2	2×	297.78(2)	0.214	0.274
Sn1−Sn2	1×	321.29(4)	0.295	0.239
Sn1−Sn2	1×	325.82(5)	0.173	0.201
Sn1−Sn1	2×	332.34(3)	0.211	0.156
Sn1−Sn2	2×	361.33(3)	0.040	0.051
Sn1−Sn1	2×	366.53(5)	0.052	0.042
Sn1−Sn1	2×	386.83(3)	−0.006	0.019
Sn2−Sn3	2×	337.97(3)	0.136	0.126
Sn2−Sn3	2×	343.53(4)	0.123	0.102
Sn2−Sn2	2×	387.81(3)	−0.014	0.019
Sn3−Sn3	2×	297.78(2)	0.348	0.589
Sn3−Sn3	2×	360.95(3)	0.079	0.052

distances of 180 pm to the vertexes (Sn3) and 220 and 289 pm to the Ti and Sn atoms in the equatorial plane of the octahedra. It is assumed that Sn-based valence electrons fill these spheres.

The Ti1, Sn2, and Sn3 atoms are surrounded by 11 other atoms, like Ti2, if one includes all interatomic distances shorter than 350 pm (Table 4), whereas Sn1 is coordinated by 5 Ti and 4 Sn atoms, forming a rather irregularly shaped polyhedron, maybe described best as a severely distorted tricapped octahedron (Figure 4). Ti1 is located between a Sn_4 rectangle and a Sn_3Ti_2 pentagon, with each of both nearly planar faces being capped by yet another atom. Altogether the Ti1-centered polyhedron consists of a capped square pyramid (octahedron) and a capped pentagonal pyramid sharing a common vertex, which is occupied by the Ti1 atom. The more regular Edshammar polyhedron (a 5-fold-capped trigonal prism) is not present in the structure of Ti_2Sn_3; the Sn2-centered polyhedron is more irregular than that Ti1-centered one, while the Sn3 atom is situated in a tricapped (somewhat) distorted cube.

(23) Jouault, F.; Lecocq, P. *C. R. Acad. Sci.* **1965**, *260*, 4777.
(24) Ellis, T. G.; Wilhelm, H. A. *J. Less-Common Met.* **1964**, *7*, 67; Jouault, F.; Lecocq, P. *Colloq. Int. CNRS* **1967**, *157*, 229.
(25) Hollan, L.; Lecocq, P.; Michel, A. *C. R. Acad. Sci.* **1964**, *258*, 3309.
(26) Wölpl, T.; Jeitschko, W. *J. Alloys Compd.* **1994**, *210*, 185.
(27) Schwomma, O.; Nowotny, H.; Wittmann, A. *Monatsh. Chem.* **1964**, *95*, 1538.

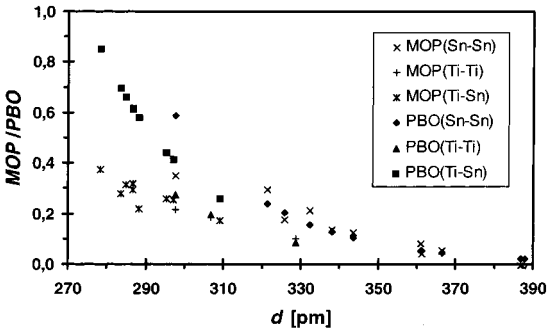

Figure 5. Overview of all interatomic interactions <400 pm.

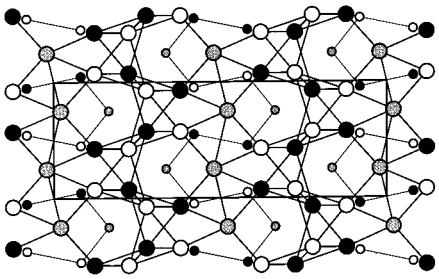

Figure 6. Projection of the structure of Ti_2Sn_3 along [100], emphasizing the homonuclear interactions. Horizontal: *b* axis. Small circles, Ti; large circles, Sn. The different heights are reflected in different shadings of the atoms.

While the heteronuclear Ti−Sn bonds outweigh the homonuclear ones by far with respect to multitude and shortness, homonuclear Ti−Ti and Sn−Sn interactions are definitely present in the structure of Ti_2Sn_3. This coincides well with the difference in electronegativity between the constituent elements (e.g., Allred and Rochow electronegativities: Ti, 1.32; Sn, 1.72; or Pauling: 1.5 vs 1.8), which indicates a charge transfer from the Ti to the Sn atoms, and polar Ti−Sn interactions.

The Ti−Sn bonds range from 278 to 309 pm, and the shortest Ti−Ti and Sn−Sn bonds occur in linear Ti2 and Sn3 chains, respectively, with interatomic separations of $b/2 = 298$ pm. Similarly, linear Ti and Sn chains are also exhibited in the structure of Ti_6Sn_5, where they run parallel to [001] with interatomic distances of $c/2 = 285$ pm. Comparable Ti and Sb chains occur in the structure of (Zr,Ti)Sb, again running parallel to the *c* axis with $d = c/2 = 284$ pm, while larger Ti−Ti distances (315 pm) were found in the linear Ti chain of TiSb (NiAs type). Band structure calculations revealed the Sb−Sb interactions in the linear Sb chains of $(Zr,V)_{13}Sb_{10}$[28] and $(Zr,V)_{11}Sb_8$[29] to be (delocalized) one-electron-two-center σ bonds, i.e., having a bond order of $^1/_2$, although the lengths of ca. 284 pm correspond to typical single bonds.

However, the shortest Ti−Sn distances are close to the sums of the Pauling single-bond radii of $r_{Ti} = 132$ and $r_{Sn} = 142$ pm,[30] compared to bond orders of 0.27 (Ti2−Ti2) and 0.59 (Sn3−Sn3) of the shortest homonuclear interactions, using Pauling's equation $d(n) = d(1) - 60$ pm $\times \log n$ (with n = Pauling bond order, PBO). Note that the bond order of the Sn3−Sn3 bond is very close to the value of $^1/_2$, as expected based on the calculations in the case of the antimonides mentioned above. The Mulliken overlap populations (MOPs), which serve as a tool to estimate relative bond strengths, are positive for all interatomic distances in Ti_2Sn_3 < 370 pm, which correspond to positive overlap and thus bonding character. The strong correlations between bond lengths and strengths in Ti_2Sn_3 are revealed in Figure 5. A notable exception is related to the beforementioned strength of the short Sn3−Sn3 bond.

Taking all Ti−Ti bonds < 330 pm and all Sn−Sn bonds < 370 pm into consideration, one observes a three-dimensional extended Sn network which includes Ti layers, as emphasized in Figure 6. As suggested by the Mulliken overlap populations, the Sn−Sn interactions between 361 and 367 pm still have significant bonding character, with overlap populations between 0.04 and 0.08, compared to 0.35 of the stronger Sn−Sn bond with a bond order of presumably $^1/_2$. The same is true for the Ti−Ti bonds between 298 and 329 pm with MOPs between 0.21 and 0.10. Comparing the latter to the Ti−Ti bonds in (Zr,Ti)Sb ($d = 284$ pm, MOP = 0.27),[1] in TiSb ($d = 315$ pm, MOP = 0.16), or in elemental titanium ($d = 289/293$ pm, MOP = 0.23/0.21).[31] Ti−Ti bonding in Ti_2Sn_3 is definitely strong as well.

In an attempt to assign oxidation states to the atoms in Ti_2Sn_3, we consider all electrons from the Ti atoms transferred to the Sn atoms, except for the ones used for Ti−Ti bonding. The sums of the Ti−Ti Pauling bond orders for Ti1 are 0.474≈0.5 and for Ti2 are 0.938≈1, while the Mulliken overlap populations gave a comparable ratio (0.468:0.796)—note that the MOPs can serve only as a relative measure for the evaluation of bond orders. Using the PBOs for electron counting, we assign maximal oxidation states of +3.5 for Ti1 and +3 for Ti2, resulting in a reduction of the three Sn atoms with 6.5 electrons. To estimate the distribution of these electrons among the three Sn atoms, we calculate the total Sn−Sn Pauling bond orders to be 0.938 for Sn1, 0.998 for Sn2, and 1.738 for Sn3 (including all Sn−Sn distances <370 pm). Thus, the Sn atoms could be reduced by roughly three (Sn1 and Sn2) and two (Sn3) electrons, respectively, if available. The formulation $Ti^{+3.5}Ti^{+3}(Sn^{-2.5})_2Sn^{-1.5}$ appears to be the most accurate one, although it remains a crude approximation only. This assignment, however, readily explains the occurrence of homonuclear bonds of both kinds, i.e., Ti−Ti and Sn−Sn bonds.

Electronic Structure. The densities of states (DOS), as calculated with the LMTO method, are shown in Figure 7. The valence band may be divided into two overlapping areas, the lower one being dominated by Sn *p* states and the upper one by Ti *d* states. The Fermi level E_F, being dominated by Ti contributions, falls close to a pronounced local minimum, but nevertheless a significant number of states are filled at E_F. Since no band gap is present in the vicinity of E_F, even heavy doping would not result in a transition to the semiconducting state.

The COHP curves (COHP: crystal orbital Hamiltonian populations[32]) show that only bonding states are filled in the cases of the Ti−Sn and Ti−Ti interactions, whereas antibonding Sn−Sn states start to get filled at

(28) Kleinke, H. *J. Chem. Soc., Chem. Commun.* **1998**, 2219.
(29) Kleinke, H. *J. Mater. Chem.* **1999**, *9*, 2703.
(30) Pauling, L. *The Nature of the Chemical Bond*, 3rd ed.; Cornell University Press: Ithaca, NY, 1948.
(31) Kleinke, H. Unpublished calculations.
(32) Dronskowski, R.; Blöchl, P. *J. Phys. Chem.* **1993**, *97*, 8617.

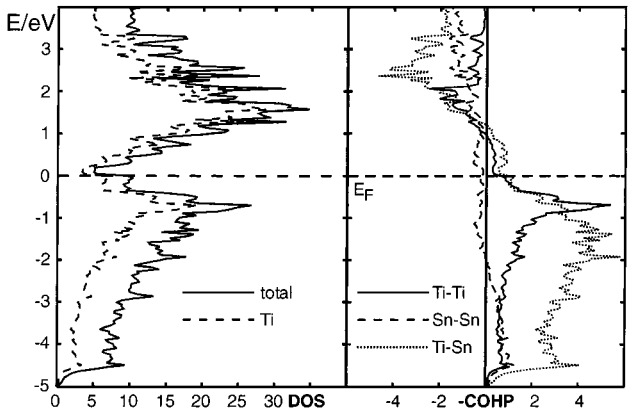

Figure 7. DOS and COHP curves of Ti_2Sn_3.

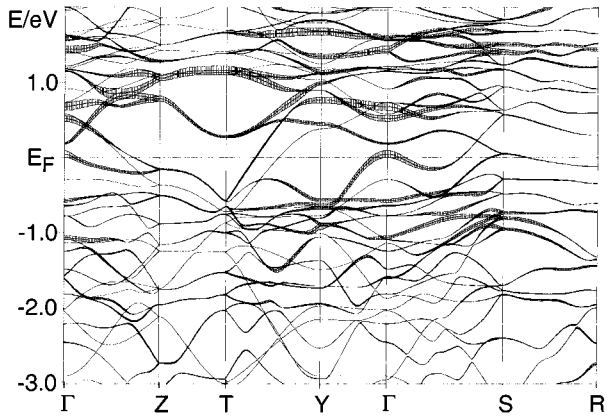

Figure 8. Band structure of Ti_2Sn_3, emphasizing via *fat band representation* of the Ti1 d_{z^2} contributions. Symmetry points: $\Gamma = (0, 0, 0)$; $Z = (0, 0, {}^1/_2)$; $T = (0, {}^1/_2, {}^1/_2)$; $Y = (0, {}^1/_2, 0)$; $X = ({}^1/_2, 0, 0)$; $S = ({}^1/_2, {}^1/_2, 0)$; $R = ({}^1/_2, {}^1/_2, {}^1/_2)$; $U = ({}^1/_2, 0, {}^1/_2)$ in units of the reciprocal lattice.

2 eV below E_F. However, a small increase of the number of the valence electrons (i.e., raising the Fermi level) would most likely lead to an overall gain in bonding interactions because of the filling of many more bonding Ti−Sn and Ti−Ti states, compared to the minor increase in antibonding Sn−Sn interactions.

To gain more insight into the properties to be expected, the band structure itself (Figure 8, special points selected according to Bradley and Cracknell[33]) has to be discussed. First, metallic properties are most likely, as several bands cross E_F along different directions, including the lines parallel to b^*, c^*, and (a^*, b^*, 0). Second, the band structure in general is interesting with respect to superconductivity because of the presence of rather dispersive bands at E_F (e.g., along the symmetry line $T-Y$ which runs at the zone border parallel to c^*) as well as two saddle points (at the zone center Γ and at S) close to the Fermi level. In contrast to $SrSn_3$, the latter cannot be deduced to arise from lone pairs of the Sn atoms since the *fat band representation*[34] reveals the corresponding band at Γ was mainly Ti1 d_{z^2} character (at S: Ti1 d_{xy} character), resembling the electronic

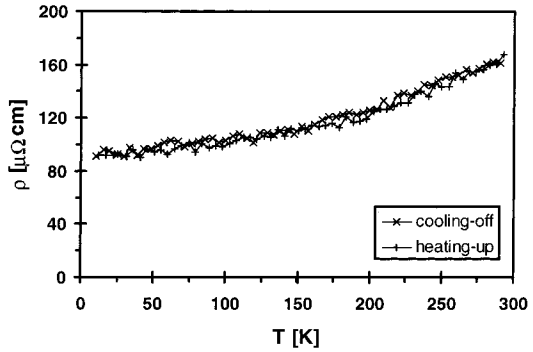

Figure 9. Specific electrical resistivity of Ti_2Sn_3.

situation in $Nb_{21}S_8$, which was recently reported to become superconducting around 4 K.[35]

The band structure of Ti_2Sn_3 complies with the chemically necessary requirements for superconductivity, i.e., the coexistence of flat and highly dispersive bands.[10] The exact location of the saddle point closest to E_F, however, is 0.05 eV above the Fermi level, which might be too far off to favor a transition to the superconducting state.

Physical Properties. The metallic character of Ti_2Sn_3, as predicted above, was experimentally confirmed by the measurements of the electrical conductivity, thermopower, and magnetic susceptibility. All of these yielded results typical for metallic compounds, namely, a specific resistivity of 160 μΩ cm at room temperature, which decreases smoothly with decreasing temperature (Figure 9), and a temperature-independent, slightly positive magnetic susceptibility of 4.5×10^{-3} emu/mol at an external field of 1 T, which is indicative of itinerant electrons (Pauli paramagnetism). The specific resistivities of the constituent elements in their metallic elemental states (Ti, 42; β-Sn, 11 μΩ cm) are significantly lower, which might in part be due to the grain boundaries in Ti_2Sn_3, but of a comparable order of magnitude. The small Seebeck coefficient of +0.8(1) μV/K (at 295 K) is typical for *p*-type metals and indicates that the conductivity is dominated by holes as the charge carriers. Comparable values are exhibited by several metallic elements (e.g., Sn, +1; V, +1.5; Tl, +0.3 μV/K), while titanium shows a Seebeck coefficient of +9 μV/K.[36]

To check for a possible transition to the superconducting state below 10 K, which is the lowest temperature achievable during the resistivity measurements, low-field magnetic susceptibility measurements were carried out at 50 G down to 1.8 K. Bulk superconductivity is known to reflect itself in a transition into an ideal diamagnetic state, which did not take place under the reaction conditions used. That Ti_2Sn_3 is no superconductor could be due to the location of the van Hove singularity 0.05 eV above E_F or simply to the fact that the presence of the chemical band structure fingerprint cannot serve as a proof for superconductivity. Since the Fermi level could be raised by a partial substitution of Ti by Nb or of Sn by Sb, i.e., adding roughly 0.2 valence electrons per formula unit would bring the Fermi level

(33) Bradley, C. J.; Cracknell, A. P. *The Mathematical Theory of Symmetry in Solids*; Clarendon Press: Oxford, 1972.
(34) Jepsen, O.; Andersen, O. K. *Z. Phys.* **1995**, *97*, 25.
(35) Köckerling, M.; Johrendt, D.; Finckh, E. W. *J. Am. Chem. Soc.* **1998**, *120*, 12297.
(36) Rowe, D. M. *CRC Handbook of Thermoelectrics*; CRC Press: Boca Raton, FL, 1995.

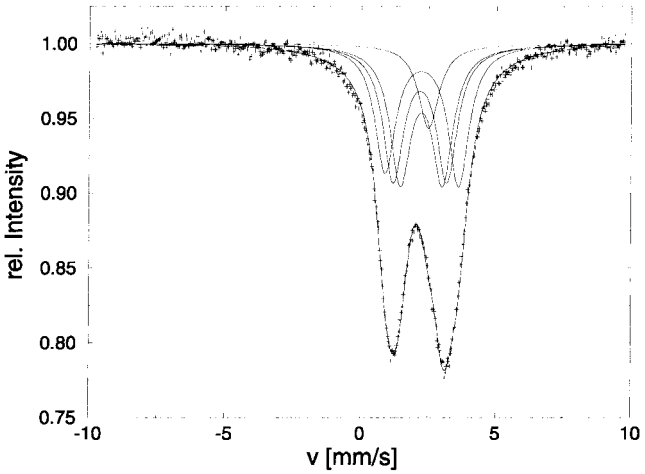

Figure 10. Experimental and simulated ^{119}Sn Mössbauer spectrum of Ti_2Sn_3, recorded at 100 K.

Table 5. Results of the Mössbauer Investigations at T = 100 K ($Ca^{119}SnO_3$ Source at 295 K)

species	isomer shift (mm/s)	quadrupole splitting (mm/s)
a	2.19	1.98
b	2.24	1.55
c	2.26	2.72

directly to the saddle point at Γ, we will investigate the substitution chemistry of Ti_2Sn_3 to further investigate the superconductivity topic.

To support the classification of Ti_2Sn_3 as a stannide and to gain more information about the three crystallographically independent Sn atoms, Mössbauer spectra were recorded at 295 and 100 K. No significant differences were found between these two Mössbauer spectra, the latter being presented in Figure 10. The spectra were fitted with four different species, three for the three Sn sites in Ti_2Sn_3 and one for a minor impurity. Under the supposition of equal Debye−Waller factors, the impurity concentration, identified based on the isomer shift of 2.5 mm/s as β-Sn, was approximately 5%.

An assignment of the different Sn species to the crystallographic sites is not straightforward; however, the occurrence of three different doublets (Table 5) demonstrates minor chemical differences between Sn1, Sn2, and Sn3. The deformation of one doublet is assigned to arise from texture effects. Only one doublet was found in the spectrum of $CeRu_4Sn_6$[37] with an isomer shift of $\delta = 2.00$ mm/s and a quadrupole splitting of $\Delta E_Q = 1.98$ mm/s, despite the presence of the different Sn sites. The averaged isomer shift of the three Sn sites in Ti_2Sn_3 ($\delta = 2.23$ mm/s) is of the same magnitude, which is typical for metallic stannides. The quadrupole splittings (ranging from 1.55 to 2.72 mm/s in Ti_2Sn_3) are based on the low symmetry of the coordination spheres of the Sn atoms, as depicted in Figure 4. This corresponds to the trend observed in U_2M_2Sn (M = Fe, Co, Ni, Ru, Rh, Pd; $1.82 \leq \delta \leq 1.99$ mm/s), where the quadrupole splitting of the Sn atom decreases with decreasing symmetry of the U_8Sn prism from 0.75 to 0.37 mm/s.[38]

Conclusions

The exploratory investigation of the Sn-rich part of the binary Ti−Sn system by means of chemical transport revealed the presence of the hitherto unknown Ti_2Sn_3. This new compound is thermodynamically stable with respect to disproportionation into the neighboring phases Ti_6Sn_5 and Sn at temperatures below 780 °C. The new structure type of Ti_2Sn_3, which comprises a three-dimensional extended network of interconnected Sn atoms as well as layers of Ti atoms, is discussed based on the three-dimensional condensation of the capped Ti-centered square antiprism. In addition to the dominating heteronuclear polar Ti−Sn bonds, Ti_2Sn_3 is stabilized by bonding homonuclear Ti−Ti as well as Sn−Sn interactions, as revealed by the band structure calculations at the extended Hückel and LMTO levels. A rough estimate of the oxidation states under consideration of the homoatomic interactions and the electronegativity differences yielded the formulation $Ti^{+3.5}Ti^{+3}(Sn^{-2.5})_2Sn^{-1.5}$ in a crude approximation. Mössbauer investigations showed the crystallographically independent Sn sites to be chemically different, also, with isomer shifts in the range typical for Sn atoms of metallic stannides.

In agreement with the results theoretically obtained, Ti_2Sn_3 is a metallic conductor with a small Seebeck coefficient, exhibiting Pauli paramagnetism. The scopes of some bands close to the Fermi level remind one at those of some superconductors including the high-temperature superconductors based on layered cuprates, i.e., highly dispersive bands cutting the Fermi level and very flat bands (indicative of lone pairs) at the Fermi level which serve as chemical fingerprints. No transition to the superconducting state, however, was observed above 1.8 K, which might be due to the flats band located 0.05 eV above the Fermi level. Hence, investigations of the (hypothetical) series $Ti_{2-x}Nb_xSn_3$ and $Ti_2Sn_{3-x}Sb_x$ are underway to prepare a compound with the flat band directly at the Fermi level, aiming at the preparation of an anticipated superconductor.

Acknowledgment. This work was initiated at the Department of Chemistry of the University of Marburg in Germany, supported by the BMFT, DFG, and FCI. Ongoing funding from MMO and NSERC is appreciated.

Supporting Information Available: Projection of the structure of Ti_2Sn_3 along [100], anisotropic displacement factors, and structure factors. This material can be obtained free of charge via the Internet at http://pubs.acs.org.

CM000131Z

(37) Pöttgen, R.; Hoffmann, R.-D.; Sampathkumaran, E. V.; Das, I.; Mosel, B. D.; Müllmann, R. *J. Solid State Chem.* **1997**, *134*, 326.

(38) Mirambet, F.; Chevalier, B.; Fournes, L.; Gravereau, P.; Etourneau, J. *J. Alloys Compd.* **1994**, *203*, 29.